This work has been submitted to a possible publication in RAAD 2026
35th International Conference on Robotics in Alpe-Adria-Danube Region, ©Springer

# Stewart-Platform Six-DoF Haptic Joystick with Force-Feedback via Cartesian Wrench Compensation

Balint Varga[1], Indrit Gashi[1], Jianan Liu[1], Peter Galambos[2], and Imre Rudas[2]

[1] Institute of Control Systems, Karlsruhe Institute for Technology, 76131 Karlsruhe, Germany, balint.varga2@kit.edu,
[2] Antal Bejczy Center for Intelligent Robotics, Research and Innovation Center of Obuda University, Budapest, Hungary peter.galambos@irob.uni-obuda.hu

**Abstract.** This paper presents the development of a novel six-degree-of-freedom (DoF) force-feedback (FF) joystick, which is designed for controlling large mobile manipulators. We first present the joystick design based on a compact Stewart-platform mechanism to generate motion in all transnational and rotational DoF. A computationally efficient closed-form inverse-kinematics formulation is derived, and the necessary forward-kinematics solution is presented. The forward-kinematics solver is implemented on an Arduino-class microcontroller, demonstrating that the approach is suitable for embedded real-time operation. In addition, FF is provided in each DoF to support operator during manipulation. With our novel compensation scheme, the nonlinearities of the parallel mechanism are addressed to achieve a linear force-displacement characteristic, improving operator comfort. Finally, the proposed joystick is integrated into a human-in-the-loop simulator, and a control mapping is implemented exemplarily. Initial tests demonstrate the approach is feasible and suggest broad utility for future applications..

**Keywords:** Six DOF joystick; Force feedback; Haptics; Stewart platform; Parallel robot kinematics

## 1 Introduction

Mobile manipulators (MMs) are a class of robotic systems that combine a mobile base (also called *vehicle*) with a robotic arm (*manipulator*). Small MMs, along with their modeling, analysis, and control challenges, have been studied extensively in the literature; see [1], [2], [3]. These works typically target fully autonomous operation and do not consider the presence of a human operator. A further field is the large hydraulic manipulator, controlled by a human operator, which is necessary as the working environment of these systems is contaminated and unstructured and sensors work unreliably. Therefore, an automation without a human operator is not practicable in the near future; see [4], [5], [6].

The MM system considered in this work lies between these two classes of robotic systems. The mobile base is a mid-sized tractor, and the manipulator is a large

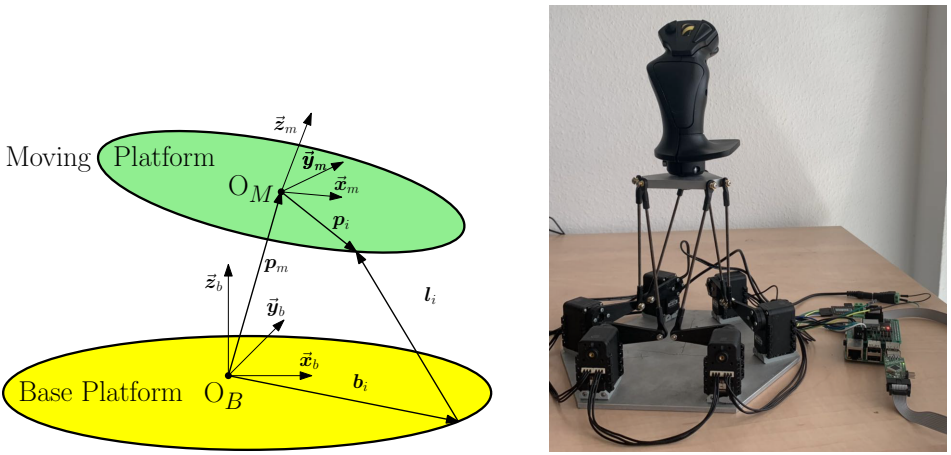


**Fig. 1:** (a) Stewart platform schematic and (b) picture of the realized system with rotary actuators.

hydraulic arm (see, e.g., [7]). Such platforms are used in roadside maintenance and in agricultural operations such as trench cleaning.

A fully automated control concept of such MMs has been proposed in [8]. In practice, however, these approaches are difficult to deploy due to unreliable sensors. To address this limitation, shared control concepts are proposed in which the automation controls only the mobile base to assist the operator, who directly controls the manipulator; see [9] or [10]. The method relies solely on operator commands, requiring no manipulator state measurements or reference trajectory.

In this work, we propose a compact Stewart Platform (SP)-based six-DoF joystick for controlling a mobile manipulator, using rotary actuation and embedded computation. The contributions of this work are: (i) a compact SP-based 6-DoF joystick with rotary actuation for embedded real-time control, (ii) an Arduino-class forward-kinematics implementation for real-time pose estimation, and (iii) a Cartesian-wrench compensation method for near-linear, direction-independent haptic stiffness.

## 2 The proposed six-DoF joystick

### 2.1 Application context and joystick mechanism

Hydraulic manipulators are widely used due to their high power-to-weight ratio and robustness to contamination [4]. In practice, such machines are commonly operated with 2-DoF joysticks that command joint or task-space velocities (rate control). To extend operator input and enable haptic cues while preserving the robustness of rate control, we realize the joystick as a compact Stewart platform

(SP) [11]. The SP is a six-legged parallel mechanism connecting a base platform (BP) and a moving platform (MP) (Fig. 1a), offering high stiffness/load capacity and a naturally limited workspace [12], consistent with conventional operating elements [4].

### 2.2 Kinematics of the Stewart Platform

A schematic of the SP is shown in Fig. 1a. For parallel robots, inverse kinematics (IK) are typically available in closed form [12]. For a desired platform pose $\boldsymbol{x}$ defined by position $\boldsymbol{p}_m$ and orientation ${}^B\mathbf{R}_M$, the $i$-th leg vector $\boldsymbol{\ell}_i$ and its length $l_i$ in the base-platform (BP) frame $\mathcal{F}_B$ are computed as:

$$\boldsymbol{\ell}_i(\boldsymbol{x}) = \boldsymbol{p}_m + {}^B\mathbf{R}_M \boldsymbol{b}_i - \boldsymbol{p}_i, \quad l_i(\boldsymbol{x}) = \|\boldsymbol{\ell}_i(\boldsymbol{x})\|, \tag{1}$$

where ${}^B\mathbf{R}_M$ maps the MP frame $\mathcal{F}_M$ to $\mathcal{F}_B$. Vectors $\boldsymbol{b}_i$ and $\boldsymbol{p}_i$ denote attachment points in $\mathcal{F}_M$ and $\mathcal{F}_B$, respectively, for $i \in \{1, \ldots, 6\}$. Following [13], our system utilizes fixed rotary actuators where motor angles $\boldsymbol{\varphi} = [\varphi_1, \ldots, \varphi_6]^T$ are determined by the actuator geometry $\boldsymbol{\varphi} = \boldsymbol{g}(l_1, \ldots, l_6)$; see Fig. 1b.

Forward kinematics (FK) determine the pose $\boldsymbol{x}$ from measured angles $\boldsymbol{\varphi}$ by first computing leg lengths $l_i(\boldsymbol{\varphi})$ and then solving the loop-closure constraints. We define a residual vector $\boldsymbol{f}(\boldsymbol{x}) \in \mathbb{R}^6$ with components:

$$f_i(\boldsymbol{x}) = \boldsymbol{\ell}_i(\boldsymbol{x})^T \boldsymbol{\ell}_i(\boldsymbol{x}) - l_i(\boldsymbol{\varphi})^2 = 0. \tag{2}$$

The pose is estimated by solving $\boldsymbol{f}(\boldsymbol{x}) = \mathbf{0}$ via Newton–Raphson iteration:

$$\boldsymbol{x}_{k+1} = \boldsymbol{x}_k - \big(J_f(\boldsymbol{x}_k)\big)^\dagger \, \boldsymbol{f}(\boldsymbol{x}_k), \tag{3}$$

where $J_f = \partial \boldsymbol{f} / \partial \boldsymbol{x}$ and $(\cdot)^\dagger$ is the pseudoinverse. Upon convergence, $\boldsymbol{x}$ represents the estimated joystick pose.

The commercially available 2-DoF operating elements are typically stabilized about their center by a linear spring–mass characteristic: larger displacements from the center produce proportionally larger restoring forces. To realize this behavior, the motor torques are commanded as

$$\boldsymbol{\tau}_i = c_{\text{ang}} \cdot \Delta\varphi_i, \tag{4}$$

where $\Delta\varphi_i$ is the deviation of the motor angles from the desired angles and $c_{\text{ang}}$ is the spring constants. Using rotatory actuators raise the following problem: Setting of the desired position with (4) causes non-linear forces on the joystick. To enable linear behaviour, a spring equation for the position and orientation of the joystick must be used with the following equation $\boldsymbol{F} = c_{\text{pos}} \cdot \Delta\boldsymbol{x}$, where $\boldsymbol{F} = [f_x, f_y, f_z, \tau_x, \tau_y, \tau_z]$ is the wrench with the force and torque components of the joystick grip. The deviation from the desired position and orientation of the joystick is $\Delta\boldsymbol{x}$ and $c_{\text{pos}}$ is the new spring constant. Computing the desired wrench, the so call static wrench transmission of the closed chain is computed [14]

$$\boldsymbol{\tau}_i = J^T \boldsymbol{\tau}. \tag{5}$$

This Cartesian-wrench formulation is the basis for the compensation concept described next.

## 3 The proposed control concepts

### 3.1 Design of the haptic feedback

When designing the haptic feedback, human haptic perception must be considered to ensure comfortable joystick operation and a seamless human-machine interaction [16]. In particular, the rendered wrench should be reliably perceivable at the hand (i.e., above absolute detection thresholds) and should change in increments that exceed the differential threshold (just-noticeable difference) [15]. The absolute threshold $\Omega_0$ denotes the minimum stimulus magnitude required for perception; for palmar contact, reported force thresholds are in the low-millinewton range. Moreover, perceived intensity is often modeled as logarithmic in the stimulus magnitude according to the Weber-Fechner relation,

$$E = c \ln\left(\frac{\Omega}{\Omega_0}\right),$$

where $c$ depends on the stimulus type [15]. Accordingly, the controller applies component-wise lower bounds to the commanded force and moment components so that the rendered cues remain perceptible and are not dominated by quantization and friction effects. Moments are expressed consistently with the handle geometry by relating them to an effective grip moment arm.

### 3.2 Design of the control concept

To highlight the benefits of the proposed approach, four DoFs of the joystick are used to enable an intuitive human-machine interaction. A standard 2-DoF joystick typically provides two rotational inputs about the $x$- and $y$-axes. The proposed joystick allows flexible DoF allocation: some DoFs command the manipulator, while others render vehicle-state haptic cues.

In the conventional 2-DoF concept, the desired joystick pose is the origin, $\boldsymbol{x} = \mathbf{0}$. The operator feels only a linear centering spring characteristic, i.e., no active forces are rendered. The manipulator is controlled using coordinated rate control: the joystick rotations are mapped to end-effector velocity commands,

$$\dot{x}_{\text{manip}} = K_x \cdot \beta_{\text{joy}} \text{ and } \dot{y}_{\text{manip}} = K_y \cdot \alpha_{\text{joy}},$$

where $K_x$ and $K_y$ are parameters determined by the manipulator inverse kinematics. The proposed concept uses a different mapping. Here, the joystick translations in $x$ and $y$ are mapped to the manipulator velocity commands,

$$\dot{x}_{\text{manip}} = K_x^* \cdot x_{\text{joy}}, \text{ and } \dot{y}_{\text{manip}} = K_y^* \cdot y_{\text{joy}}, \tag{6a}$$

where $K_x^*$ and $K_y^*$ again depend on the inverse kinematics. In addition, two rotational DoF are set by the automation to represent the current vehicle velocity and steering angle,

$$\beta_{\text{joy}} = K_{\text{v,veh}} \cdot v_{\text{veh}}, \text{ and } \gamma_{\text{joy}} = K_{\delta_{veh}} \cdot \delta_{\text{veh}}, \tag{7a}$$

thereby providing the operator with a haptic indication of the vehicle state. The remaining DoF have the same desired values as in the conventional concept, $[x_{\text{joy}}, y_{\text{joy}}, z_{\text{joy}}, \alpha_{\text{joy}}] = [0, 0, 0, 0]$. The mapping of the proposed concept is illustrated in Fig. 2.

### 3.3 Feedback Force Generation

The following subsection summarizes the proposed force-feedback generation method. The key motivation is that rendering stiffness and force feedback (FF) purely from motor-side quantities can reduce usability, since the resulting force levels can vary significantly with direction.

To avoid this, the joystick is treated as a single system and a Cartesian wrench $\boldsymbol{F}$ is defined from the current tool center point (TCP) pose $\boldsymbol{x}_{is}$ toward a configurable rest pose $\boldsymbol{x}_{des}$. The wrench consists of a force vector and a moment vector applied at the TCP. To obtain trajectories that feel natural, the concept follows curved paths by defining a next pose $\boldsymbol{x}_{next}$ on the TCP trajectory and rendering forces tangentially along this path. Thus, the Cartesian force and moment are computed as

$$\mathbf{F}_{xyz} = \left(k_1 + k_2 \left\|x_{\text{des,pos}} - x_{\text{is,pos}}\right\|\right) \frac{x_{\text{next,pos}} - x_{\text{is,pos}}}{\left\|x_{\text{next,pos}} - x_{\text{is,pos}}\right\|} \text{ and} \tag{8}$$

$$\mathbf{T}_{\alpha\beta\gamma} = \left(k_3 + k_4 \left\|x_{\text{des,orient}} - x_{\text{is,orient}}\right\|\right) \frac{x_{\text{des,orient}} - x_{\text{is,orient}}}{\left\|x_{\text{des,orient}} - x_{\text{is,orient}}\right\|}, \tag{9}$$

where $k_1$, $k_2$, $k_3$, and $k_4$ are tunable stiffness parameters for the force and moment components, respectively. Both components are combined into the wrench

$$\boldsymbol{\tau} = \begin{pmatrix} \mathbf{T}_{\alpha\beta\gamma} \\ \mathbf{F}_{xyz} \end{pmatrix}, \tag{10}$$

which is applied to (5).

## 4 Simulator Integration and Results

### 4.1 The simulator of the MM

The joystick operates a large MM system. Vehicle dynamics follow [17], and the hydraulic manipulator model (four cylinders, four arm segments) is based on [18]. The operator commands end-effector velocity, which is converted to joint inputs via inverse kinematics. The simulator includes a GUI that displays an offline-computed manipulator reference trajectory for the operator to track. Using the proposed joystick, the operator attempts to follow the reference trajectory as closely as possible. The simulator runs in real time on a standard PC, and the joystick is connected via a microcontroller that handles the kinematics and FF computations.

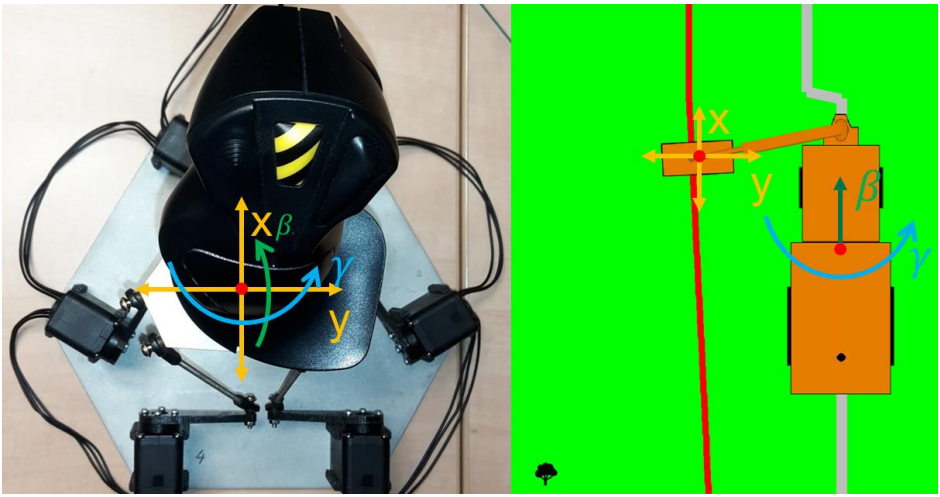


**Fig. 2:** Stewart-platform joystick mapping: translations command the manipulator, rotations present vehicle state as haptic cues.

### 4.2 Result and discussion of the compensation

The main result of the compensation is the linear force-feedback characteristics of the joystick. Fig. 3 compares force-displacement curves obtained with motor-space stiffness (*old concept*) and with the proposed Cartesian-wrench compensation (*novel concept*). The compensated measurements closely follow the desired linear spring behavior, whereas the uncompensated curves exhibit kinks and deviations at large displacements. The working space is comparable to conventional joysticks: translation ranges of $\pm 60\,\mathrm{mm}$ in $X/Y$ and $\pm 45\,\mathrm{mm}$ in $Z$, rotation ranges of $\pm 50^\circ$ in pitch/roll and $\pm 40^\circ$ in yaw, with full force/torque rendering over approximately 10 cm translation and $15^\circ$ rotation at a maximum of 1.5 N m per servo.

Several factors influence the measured profiles beyond the control law itself. First, the two concepts were recorded over different displacement intervals: with motor-angle stiffness, the configuration-dependent transmission can cause rapidly increasing grip forces, restricting a sweep range due to too high forces, whereas the Cartesian-wrench approach specifies stiffness at the grip and thus permits a larger workspace. Second, slight offsets around the neutral position are expected due to assembly tolerances and load-dependent friction; these should be mitigated in future work. Since the displacement was increased manually during the measurement, small fluctuations occur near the end of the operating range; these can be improved with advanced signal filtering. A conclusive comparison will include additional quantitative metrics over a common interval to separate controller effects from measurement and hardware artifacts. An additional benefit of the current design lies in the cost efficiency compared to the other state-of-the-art 6-DoF haptic devices, see e.g. [19].


**Fig. 3:** Force-displacement characteristics after compensation

## 5 Conclusion and outlook

This paper presents a novel six-DoF joystick for controlling large mobile manipulators. The joystick uses a Stewart-platform mechanism, and its kinematics are solved using closed-form inverse kinematics and an iterative forward-kinematics approach. A compensation method is developed to provide linear FF to the operator. The joystick is integrated into a simulator of a large MM, and two control mappings are implemented. Initial tests demonstrate the feasibility of the approach and highlight its potential for improving operator performance and comfort.

## References

1. Ji-Chul Ryu and Sunil K. Agrawal. Planning and control of under-actuated mobile manipulators using differential flatness. *Auton Robot*, 29(1):35–52, July 2010.
2. Pal Johan From. *Vehicle-Manipulator Systems: Modeling for Simulation, Analysis, and Control*. Advances in Industrial Control. Springer, New York, 1st edition edition, 2013.
3. M. Mashali, R. Alqasemi, and R. Dubey. Task priority based dual-trajectory control for redundant mobile manipulators. In *2014 IEEE International Conference on Robotics and Biomimetics (ROBIO 2014)*, pages 1457–1462, Bali, Indonesia, December 2014. IEEE.
4. Bing Xu and Min Cheng. Motion control of multi-actuator hydraulic systems for mobile machineries: Recent advancements and future trends. *Front. Mech. Eng.*, 13(2):151–166, June 2018.
5. Balint Varga, Arash Shahirpour, Markus Lemmer, Stefan Schwab, and Soren Hohmann. Limited-Information Cooperative Shared Control for Vehicle-Manipulators. In *IEEE International Conference on Systems, Man, and Cybernetics (IEEE SMC 2020)*, page 8. IEEE, Piscataway, NJ, 2020.

6. I Yung, Carlos Vázquez, and Leonid B. Freidovich. Robust position control design for a cylinder in mobile hydraulics applications. *Control Engineering Practice*, 69:36–49, December 2017.
7. Balint Varga, Arash Shahirpour, Yannick Burkhardt, Stefan Schwab, and Soren Hohmann. Validation of Cooperative Shared-Control Concepts for Large Vehicle-Manipulators. In *2020 IEEE Conference on Control Technology and Applications (CCTA)*, pages 542–548, Montreal, QC, Canada, August 2020. IEEE.
8. Jouko Kalmari, Juha Backman, and Arto Visala. Coordinated motion of a hydraulic forestry crane and a vehicle using nonlinear model predictive control. *Computers and Electronics in Agriculture*, 133:119–127, February 2017.
9. Balint Varga, Arash Shahirpour, Stefan Schwab, and Soeren Hohmann. Control of Large Vehicle-Manipulators with Human Operator. *IFAC-PapersOnLine*, 52(30):373–378, 2019.
10. Balint Varga and Sören Hohmann. Limited information longitudinal shared control of large vehicle-manipulator. *IFAC-PapersOnLine*, 55(29):43–48, 2022.
11. D. Stewart. A Platform with Six Degrees of Freedom. *Proceedings of the Institution of Mechanical Engineers*, 180(1):371–386, June 1965.
12. Bruno Siciliano and Oussama Khatib. *Springer Handbook of Robotics*. Springer Berlin Heidelberg, New York, NY, 2nd edition edition, 2016.
13. Filip Szufnarowski. Stewart platform with fixed rotary actuators: A low cost design study. page 11, 2013.
14. Kenneth J. Waldron and Kenneth H. Hunt. Series-Parallel Dualities in Actively Coordinated Mechanisms. *The International Journal of Robotics Research*, 10(5):473–480, October 1991.
15. Christian Hatzfeld, Thorsten A Kern, and SpringerLink (Online service). *Engineering Haptic Devices a Beginner's Guide*. Springer London : Imprint : Springer, London, 2014.
16. Balint Varga, Frank Flemisch, and Sören Hohmann. Human in the loop. *at - Automatisierungstechnik*, 72(12):1109–1111, 2024.
17. Roland L. Kovacs, Laszlo Nadai, and Zoltan Hankovszki. Modeling of commercial vehicles for vehicle dynamics control development. In *2014 IEEE 9th IEEE International Symposium on Applied Computational Intelligence and Informatics (SACI)*, pages 305–310, Timisoara, Romania, May 2014. IEEE.
18. Michael Ruderman. Full- and reduced-order model of hydraulic cylinder for motion control. In *IECON 2017 - 43rd Annual Conference of the IEEE Industrial Electronics Society*, pages 7275–7280, Beijing, October 2017. IEEE.
19. Christian A. Braun, et al. Using a collaborative robotic arm as human-machine interface: System setup and application to pose control tasks. In *2023 IEEE International Conference on Robotics and Automation (ICRA)*, pages 12464–12470, 2023.